Aerogel as a Soft Acoustic Metamaterial for Airborne Sound

Matthew D. Guild,* Victor M. García-Chocano, and José Sánchez-Dehesa†
Wave Phenomena Group, Departamento de Ingeniería Electrónica, Universidad Politécnica de Valencia, Camino de vera s/n (Edificio 7F), E-46022 Valencia, Spain

Theodore P. Martin, David C. Calvo, and Gregory J. Orris
U.S. Naval Research Laboratory, Code 7160, Washington, D.C. 20375, USA
(Received 25 September 2015; revised manuscript received 7 March 2016; published 30 March 2016)

Soft acoustic metamaterials utilizing mesoporous structures have been proposed recently as a means for tuning the overall effective properties of the metamaterial and providing better coupling to the surrounding air. In this paper, the use of silica aerogel is examined theoretically and experimentally as part of a compact soft acoustic metamaterial structure, which enables a wide range of exotic effective macroscopic properties to be demonstrated, including negative density, density near zero, and nonresonant broadband slow-sound propagation. Experimental data are obtained on the effective density and sound speed using an air-filled acoustic impedance tube for flexural metamaterial elements, which have been investigated previously only indirectly due to the large contrast in acoustic impedance compared to that of air. Experimental results are presented for silica aerogel arranged in parallel with either one or two acoustic ports and are in very good agreement with the theoretical model.

DOI: 10.1103/PhysRevApplied.5.034012

I. INTRODUCTION

Acoustic metamaterials have received interest in recent years by enabling macroscopic physical characteristics which cannot be obtained with traditional materials, such as negative, near-zero, or anisotropic dynamic effective fluid properties. Acoustic metamaterials are able to achieve such previously unattainable exotic properties through the careful design of the microstructure, which creates microscale dynamics that results in the desired macroscopic properties. The reader is addressed to the recent reviews on this topic where one can find many of the exciting applications of acoustic metamaterials [1,2].

Until recently, such acoustic metamaterials have relied on materials which are much harder than the surrounding fluid medium, often treated as acoustically rigid or nearly rigid structures for airborne sound. Alternatively, soft acoustic metamaterials utilizing mesoporous structures have been proposed as a means for the molding and tuning of the overall properties of the resulting metamaterial, while simultaneously providing better coupling with the acoustic environment around it [3]. Building upon this concept, the use of silica aerogel as part of a compact soft acoustic metamaterial structure is examined theoretically and experimentally, yielding an interesting suite of useful yet exotic properties.

In addition to extremely large and/or negative dynamic properties, there is a wide range of interesting and exciting phenomena associated with effective properties that are near zero, particularly, those associated with *extraordinary transmission*, which can be achieved when either the effective density or wave speed approaches zero [4,5]. In the case of a density-near-zero material, the effective wave speed increases dramatically and leads to a quasistatic field within a given structure, which can exhibit a supercoupling effect through long narrow channels [6–8]. At the opposite extreme, there are also interesting effects which arise as the effective acoustic wave speed approaches zero, which is referred to as *slow sound*, the analogue of *slow light* in optics. Previous demonstrations have utilized resonant effects using either sonic crystals or detuned resonators [9–13], resulting in slow sound that occurs over a relatively narrow bandwidth. An application of slow-sound propagation was recently proposed for the improved design of acoustic absorbers by Groby *et al.* [14], in which slow sound in large slits filled with absorptive foam was used to significantly increase the low-frequency absorption in air.

One of the fundamental aspects that gives a metamaterial its exotic macroscopic properties is the dynamics of the microstructure and the resulting "hidden" degrees of freedom that it enables [15], which has been explored recently for elastic and flexural metamaterial components [16,17]. These hidden degrees of freedom are particularly important because the effective macroscopic properties of an acoustic metamaterial can be significantly different than

*matthew.guild.ctr@nrl.navy.mil
Present address: NRC Research Associateship Program, U.S. Naval Research Laboratory, Code 7160, Washington, D.C. 20375, USA.
†jsdehesa@upv.es

those of the constituent microstructural elements. When there is open flow through the structure, such as a sonic crystal lattice [18,19] or transmission-line arrangement of Helmholtz resonators [20], it is relatively straightforward to extract effective properties experimentally due to the relatively low acoustic impedance.

A formidable challenge, however, arises when obtaining the effective properties of a metamaterial sample containing elastic elements, which have acoustic impedances that are orders of magnitude greater than the surrounding fluid and at frequencies well below those typically used to obtain acoustic properties through direct time-of-flight measurements. As a result, previous works in air have either been restricted to theoretical and numerical evaluation [4,7,21–23] or limited to an indirect comparison of the metamaterial properties using experimental results for the reflected and transmitted pressure field [5,24]. In this work, we make the significant step of experimentally extracting the effective dynamic properties (density and sound speed) of these flexural metamaterial elements.

It is expected that the elasticity of the materials defining the metamaterial structure might play a fundamental role in order to understand the phenomena observed in sound transmission and reflectance through the channels defined by the structure. In fact, the role of the elastic properties is paramount for the case of structures embedded in water, as it has been recently demonstrated [25]. Although some recent work has begun to incorporate the elastic effects into the metamaterial structure, many of these designs continue to have the primary dynamic element consisting of mass-spring resonators which are affixed to an elastic plate as structural support [22,23]. Alternatively, soft acoustic metamaterials represent a paradigm shift beyond this framework by creating the dynamics from the structure itself. It is important to emphasize that such a soft acoustic metamaterial realized with the unique properties of aerogels can be tailored to obtain a wide spectrum of desirable exotic properties in a single versatile subwavelength acoustic metamaterial element.

In this paper, theoretical and experimental results for a compact metamaterial configuration are presented. With an extremely low effective sound speed and subwavelength size, these soft acoustic metamaterial structures can be used to create a large thin arrangement with the same exotic effective properties, which can be preserved through distortion or deformation onto an arbitrary surface, thereby enabling conformal configurations. In particular, these structures represent a soft acoustic metamaterial, which is realized using the flexural resonance of the zeroth-order antisymmetric Lamb-wave mode in silica aerogel disks. In addition to its subwavelength thickness, extreme effective properties are demonstrated across a broad range of the operating bandwidth, with distinct regions exhibiting negative density, density near zero, and ultralow sound speeds.

II. BACKGROUND ON AEROGELS

While the exceptional thermal properties of aerogel have led to a revolution in thermal insulation applications, utilization of the unique acoustic characteristics has been minimal, primarily relating to marginal improvements of existing concepts such as quarter-wavelength impedance matching or ultrasonic absorbers [26–28]. However, aerogels offer several unique features that enable them to function as a subwavelength flexural element in a soft acoustic metamaterial, which is made possible by their unique microstructure. One of the most common types of aerogels, silica aerogel, consists of a high-porosity frame made of fused silica nanoparticles. The most notable characteristic of silica aerogel is its extremely low static density which is directly related to the very high porosity of the structure, making it much closer to that of air compared with any other type of elastic solid. Because of the nanoscale pore size, however, the air is locked in place by viscous effects producing a higher acoustic density than that compared to typical porous media used in acoustic applications [29]. Furthermore, the small cross section connecting the fused nanoparticles results in a very low elastic stiffness compared with a rigid silica structure of the same porosity [30]. This combination gives a relatively low acoustic impedance (for an elastic solid) and, in particular, yields an exceptionally low flexural wave speed, making it ideal for use as a subwavelength flexural element for airborne sound.

When the wavelength is much larger than the microstructure, negative effective properties are achieved via control of the microstructure arrangement and the resulting dynamics. This feature in the microstructure design is typically achieved with two main types of arrangements: either as a mass-spring system or in a transmission line consisting of mass and stiffness elements. The mass-spring systems, which demonstrate extreme effective mass and stiffness in the vicinity of the mass-spring resonance, are, therefore, referred to as *locally resonant acoustic metamaterials* (LRAMs) [5,31–35]. Although such mass and spring elements can be arranged in a compact configuration and are relatively simple and robust, the resulting extreme effective properties are inherently narrow band and subject to appreciable loss due to the close proximity of the mass-spring resonance [8,36]. Alternatively, acoustic metamaterials have been proposed using thin elastic plates as a means for operating as a positive stiffness element in acoustic transmission-line arrangements [21], which has recently been applied to acoustic metamaterial leaky-wave antennas [37]. While the unit cell of such an arrangement is much smaller than a wavelength, the entire configuration requires many elements in series and can result in a very long structure relative to the wavelength.

In this work, we employ hydrophobic silica aerogel which has a static density of 107 kg/m^3 and an (optical) refractive index of 1.03. This silica aerogel has a high

resistance for water and moisture due to its hydrophobicity, a feature allowing the disks to be fabricated using water-jet cutting techniques. Their properties are stable in any climate, a feature contributing the high reliability for the analysis provided below.

III. THEORETICAL FORMULATION

In many acoustic metamaterial configurations including LRAMs and acoustic transmission-line arrangements, thin elastic disks and membranes are used as subwavelength stiffness elements. This ubiquitous implementation arises from the fact that the time-harmonic displacement of an elastic disk is proportional to the flexural stiffness in the quasistatic (low-frequency) limit and, therefore, yields an analogous inductive behavior equivalent to that of a mechanical spring. In general, however, the specific acoustic impedance of a lossless elastic plate can be expressed in terms of the mass per area M_{plate} and compliance C_{plate} as [38]

$$Z_{\text{plate}} = j\omega M_{\text{plate}} + \frac{1}{j\omega C_{\text{plate}}} = j\omega M_{\text{plate}}\left[1 - \left(\frac{\omega_{\text{res}}}{\omega}\right)^2\right] \equiv j\omega M_{\text{eff}}(\omega), \quad (1)$$

where $\omega_{\text{res}} = (M_{\text{plate}} C_{\text{plate}})^{-1/2}$ is the angular resonance frequency of the plate. Written in this form, it is apparent that the stiffness-controlled response of the elastic plate can equivalently be treated as a frequency-dependent effective mass M_{eff}, which is negative for $\omega < \omega_{\text{res}}$.

For canonical shapes and idealized boundary conditions, analytic expressions are developed to describe the flexural wave motion of elastic solids. For the flexural motion of thick plates, effects from shear deformation and rotational inertia become important, which can be formulated using Mindlin theory [39]. For flexural waves in a thick circular elastic disk, the modal displacement w_n of the plate is given by [40,41]

$$w_n(r,\theta) = \left[A_1 J_n\left(\delta_1 \frac{r}{a}\right) + A_2 I_n\left(\delta_2 \frac{r}{a}\right)\right]\cos(n\theta), \quad (2)$$

$$\delta_1^2 = \frac{1}{2}\lambda^4\left[(R+S) + \sqrt{(R-S)^2 + 4\lambda^{-4}}\right], \quad (3)$$

$$\delta_2^2 = \frac{1}{2}\lambda^4\left[\sqrt{(R-S)^2 + 4\lambda^{-4}} - (R+S)\right], \quad (4)$$

$$R = \frac{1}{12}\left(\frac{h}{a}\right)^2, \quad (5)$$

$$S = \frac{D}{\mu h(\kappa a)^2} = \frac{1}{6(1-\nu)\kappa^2}\left(\frac{h}{a}\right)^2, \quad (6)$$

$$\lambda^4 = \frac{\rho h a^4 \omega^2}{D}, \quad (7)$$

$$D = \frac{Eh^3}{12(1-\nu^2)}, \quad (8)$$

where J_n and I_n denote the Bessel function and modified Bessel function of the first kind, a is the plate radius, h is the plate thickness, ρ is the mass density, E is Young's modulus, μ is the shear modulus, ν is Poisson's ratio, ω is the angular frequency, and $\kappa = \pi/\sqrt{12}$ is the shear correction factor. Note that for axisymmetric loading, such as that encountered in an acoustic impedance tube, the only nonzero mode is $n = 0$.

Because of the clamped boundary conditions corresponding to $w(a) = w'(a) = 0$, the characteristic equation for the flexural resonance frequencies is given by

$$J_1(\delta_1)I_0(\delta_2) + J_0(\delta_1)I_1(\delta_2) = 0. \quad (9)$$

As observed from Eq. (1), the resonance frequency denotes a critical point in the effective acoustic properties, and even though Eq. (9) provides the exact solution, it must be solved numerically. To better understand the relationship between the material properties and dimensions of the plate and the resonance frequencies, an approximate analytic expression is sought. To proceed, it is assumed that the flexural wave numbers δ_1 and δ_2 are sufficiently high so that the large argument approximations can be used for the Bessel and modified Bessel functions, namely [42],

$$\frac{J_1(x)}{J_0(x)} \approx \tan\left(x - \frac{\pi}{4}\right), \qquad \frac{I_1(x)}{I_0(x)} \approx 1. \quad (10)$$

Even in the case of large wavelengths relative to the thickness of the plate (and, therefore, in the low-frequency limit in terms of the acoustic waves in the surrounding fluid), the flexural modes occur at frequencies where the wavelengths are on the order of the diameter of the disk or less, suggesting that the assumption above is reasonable for the case of flexural acoustic metamaterial elements investigated in this work. Note that because the ratio of the modified Bessel functions given in Eq. (10) is approximately equal to unity, the resonance frequency under these conditions depends only on δ_1. Application of the approximate expressions in Eq. (10) to Eq. (9) yields

$$\tan(\delta_1) \approx 0, \quad (11)$$

for which $\delta_1 = m\pi$ with m being a nonzero integer. Equation (3) can, therefore, be written as

$$\frac{1}{2}\lambda^4[(R+S) + 2\lambda^{-2}\sqrt{1+\Delta}] = (m\pi)^2, \quad (12)$$

where

$$\Delta = \frac{1}{4}\lambda^4(R-S)^2 = \frac{3}{144}(k_p h)^2\left[\frac{2}{(1-\nu)\kappa^2}-1\right]^2, \quad (13)$$

with $k_p = \omega/c_p$ denoting the *compressional* plate wave number with plate wave speed,

$$c_p = \sqrt{\frac{E}{\rho(1-\nu^2)}}. \quad (14)$$

Typical values of compressional plate wave speeds are usually orders of magnitude higher than flexural wave speeds, and, thus, the corresponding wave numbers are much lower. As a result, one expects that $k_p h \ll 1$ and likewise $\Delta \ll 1$, in which case, Eq. (12) can be simplified to give an expression for the flexural resonance frequency of the mth mode,

$$f_{\text{res}}^{(m)} = \frac{1}{4\pi\sqrt{3}}\frac{c_p h}{a^2}\frac{1}{R+S}\left[\sqrt{1+2(m\pi)^2(R+S)}-1\right]. \quad (15)$$

In addition to the flexural resonance frequency, the particular solution to the displacement is necessary to calculate the effective acoustic properties of the flexural disk. Assuming a time-harmonic pressure P applied across the face of the disk and assuming clamped edges, the displacement becomes

$$w(r) = \frac{P}{\rho h\omega^2}\left[\frac{I_1(\delta_2)J_0(\delta_1\frac{r}{a})+J_1(\delta_1)I_0(\delta_2\frac{r}{a})}{I_1(\delta_2)J_0(\delta_1)+J_1(\delta_1)I_0(\delta_2)}-1\right]. \quad (16)$$

Although Eq. (16) gives an expression for the displacement at any given radius r, it is actually the ensemble of the displacement over all the points on the surface which will be measured via the reflected or transmitted acoustic waves at some distance from the disk. Therefore, a more useful quantity is the spatial average of the displacement, which can be obtained from Eq. (16) such that

$$w_{\text{avg}} = \frac{P}{\rho h\omega^2}\left[\frac{2(\frac{1}{\delta_1}+\frac{1}{\delta_2})J_1(\delta_1)I_1(\delta_2)}{I_1(\delta_2)J_0(\delta_1)+J_1(\delta_1)I_0(\delta_2)}-1\right], \quad (17)$$

from which one can obtain the average acoustic impedance for a thick clamped circular plate

$$Z_{\text{plate}} = j\omega M_{\text{plate}}\left\{1-2\left(\frac{1}{\delta_1}+\frac{1}{\delta_2}\right)\times\left[\frac{J_1(\delta_1)I_1(\delta_2)}{I_1(\delta_2)J_0(\delta_1)+J_1(\delta_1)I_0(\delta_2)}\right]\right\}^{-1} \equiv j\omega M_{\text{eff}}, \quad (18)$$

where $M_{\text{plate}} = \rho h$ is the acoustic mass of the plate. Although not as obvious as the form presented in Eq. (1), the expression presented in Eq. (18) also yields a negative effective mass below the first flexural resonance of the elastic plate, which is illustrated by the red solid line in Fig. 1(a) for the case of a circular silica aerogel disk. The resulting negative effective density extends over the entire range below resonance and approaches $-\infty$ as the frequency goes to zero.

Such a highly dispersive and divergent behavior is not ideal, particularly for broadband applications or if any type of acoustic impedance matching is desired. However, this effective mass can be readily modified by placing a positive acoustic mass (such as an acoustic port consisting of an air-filled hole in the support ring) in parallel with the negative dynamic mass of the plate. The resulting frequency dependence on the effective mass density is presented in

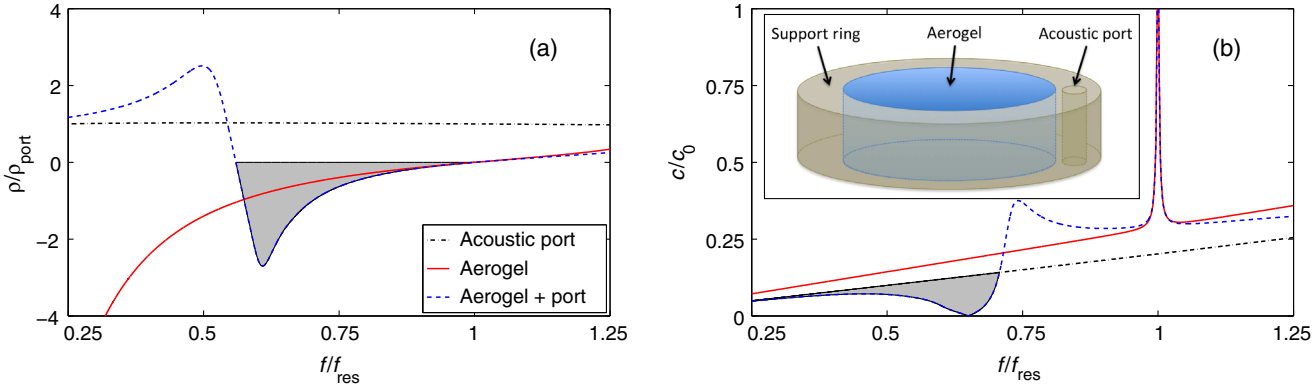

FIG. 1. Normalized plots of theoretical values of effective properties versus frequency for an aerogel disk (solid red line), an acoustic port with a rigid baffle (dash-dotted black line), and an aerogel disk combined in parallel with an acoustic port (dashed line) for (a) effective density relative to that of a baffled acoustic port and (b) effective sound speed relative to that of the surrounding fluid medium. An illustration of the parallel arrangement of the aerogel disk, baffle, and acoustic port is shown in the inset of (b), for which the effective density and sound speed are theoretically determined in (a) and (b), respectively. The shaded regions denote broadband regions of extreme effective properties, namely, (a) negative density and (b) nonresonant slow-sound propagation.

Fig. 1(a), in which a circular disk (red solid line) is combined in parallel with an acoustic port (black dash-dotted line) to obtain the effective density denoted by the dashed line. This parallel configuration of the aerogel disk and acoustic port is illustrated in the inset of Fig. 1(b). Arranged in such a manner, the acoustic port will short circuit the plate as it approaches extremely large values and allow for the magnitude and bandwidth of the negative dynamic mass (denoted by the shaded region) to be controlled using the same plate and varying only the size and number of ports.

A similar trend is observed for the effective sound speed, which is illustrated in Fig. 1(b). As in Fig. 1(a), the results for a circular elastic disk (red solid line) are arranged in parallel with an acoustic port (black dash-dotted line) to obtain the effective density denoted by the dashed line. The effective sound speed of the combined parallel arrangement follows that of the acoustic port at low frequencies, slowly decreasing towards zero before increasing again, producing a broad nonresonant region where slow-sound propagation occurs (denoted by the shaded region), slower than even that expected for the case of an acoustic port. As the frequency increases, the effective sound speed becomes dominated by the elastic disk in the vicinity of the flexural resonance of the elastic plate, which occurs at $f = f_{\mathrm{res}}$. Near this resonance, a large increase in the effective sound speed is observed as the effective density passes through zero, with the peak value limited by the losses in the system.

IV. EXPERIMENTAL SETUP

Previous approaches for the acoustic characterization of silica aerogels have been based on ultrasonic time-of-flight measurements, which have produced experimental data for the compressional and shear properties of silica aerogels [43–46]. Unfortunately, such time-of-flight measurements do not allow for one to examine the silica aerogel as part of the metamaterial structure, requiring the use of acoustic waves with wavelengths which are much smaller than the thickness of the sample for accurate time-of-flight characterization. Although most of these previous investigations involved compressional and shear waves, Rayleigh surface waves have also been examined, which were observed to be less than 50 m/s, significantly lower than the compressional wave speed [47]. Likewise, as can be seen from Fig. 1, the effective properties due to the flexural behavior of the aerogel disks at large wavelengths (low frequencies) relative to the size of the disk are dramatically different than those of the static density and compressional wave speed obtained via time-of-flight measurements for silica aerogel [43].

Alternatively, an experimental setup is needed that can examine the effective acoustic behavior of the ensemble arrangement including the silica aerogel disk, at frequencies which are sufficiently low to be within the homogenization limit for use in the microstructure of an acoustic metamaterial. The experimental investigation of the silica aerogel samples in this work is performed using an air-filled acoustic impedance tube. The experimental setup is illustrated in Fig. 2(a), which shows a standard four-microphone configuration [48] for the measurement of acoustic properties of a given sample. The acoustic properties, namely, the complex-valued acoustic impedance and wave number, are obtained as a function of input frequency from spectral measurements of the magnitude and phase of both the reflected and transmitted acoustic pressure obtained from the four microphones.

While this particular type of acoustic apparatus has been utilized for many decades, such work has traditionally focused on simply measuring transmission loss through an absorptive sample [49]. In the last several years, this technique has been expanded to acoustic metamaterials, with a particular emphasis on extraction of the effective complex acoustic properties of the acoustic metamaterial sample [19,50,51]. The method for the extraction of these properties can be found in previous works [51] based on the complex reflection and transmission pressure coefficients, which are given by

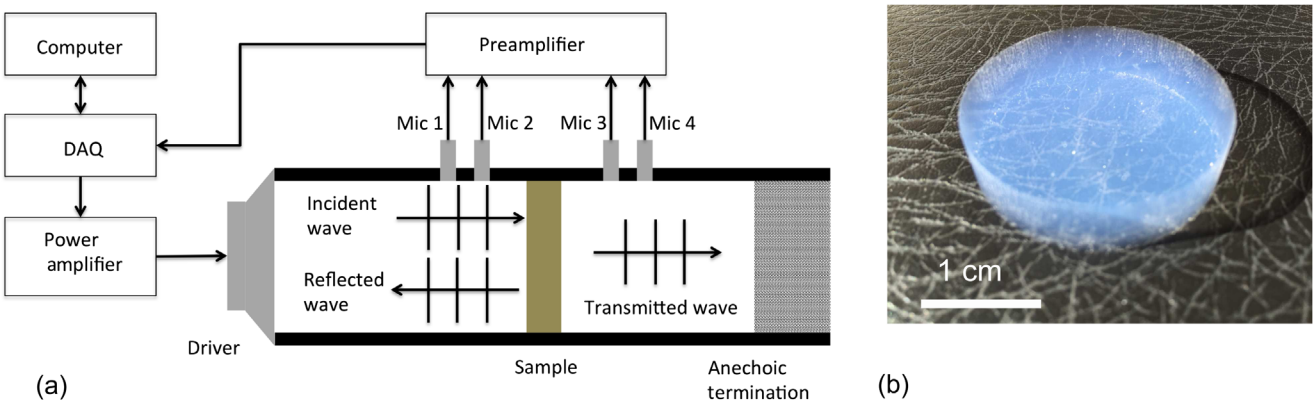

FIG. 2. (a) Diagram of the experimental setup using an air-filled acoustic impedance tube and (b) a photo of a silica aerogel sample examined in this work.

$$R_{\text{tot}} = \frac{1}{2}\frac{Z_{\text{tot}}}{Z_0}\left[1 + \frac{1}{2}\frac{Z_{\text{tot}}}{Z_0}\right]^{-1}, \tag{19}$$

$$T_{\text{tot}} = \left[1 + \frac{j\omega}{2Z_0}(M_{\text{eff}} + M_{\text{port}})\right]^{-1}, \tag{20}$$

where Z_{tot} is the total acoustical impedance seen at the face of the sample, Z_0 is the acoustical impedance of air, and M_{eff} and M_{port} are the effective acoustic mass of the aerogel disk and port, respectively.

This inverse process of using spectral acoustic measurements to obtain the complex-valued acoustic properties presents significant challenges, including ambiguity in identifying unique solutions [50] and a high sensitivity in the extracted properties to even low levels of noise in the spectral data obtained from the microphones [51]. Although these challenges have been overcome recently for samples such as sonic crystals [19,51] with a relatively low acoustic impedance relative to the surrounding air, acoustic metamaterials consisting of solid elastic structures, even relatively soft ones such as silica aerogels, with acoustic impedances hundreds of times larger than that of air present unique challenges using this technique.

As a result of this high acoustical input impedance from the sample, the small but finite leakage from the impedance tube becomes a significant source of error in the measurement and must be accounted for. Typically, this leakage is observed as a result of improper sealing and mounting of the sample, with leakage of acoustic energy from the reflected side of the sample to the transmitted side. However, in the case of rigidly mounted high-impedance samples, this leakage is primarily due to the microphones, which consist of thin diaphragms and small acoustic ports for pressure equalization, with the main source of this leakage occurring on the reflected side of the sample. As a result, two distinct differences arise for this case of microphone pressure leakage compared with that due to improper mounting: (1) the leakage occurs in the reflected pressure measurements only, with negligible effects on the transmitted side, and (2) for large impedances, the leakage should be independent of the specific sample or its particular mounting in the impedance tube.

Under these conditions, the total acoustical impedance seen at the front of the sample can be written as

$$Z_{\text{tot}} = \left[\frac{\phi_{\text{plate}}}{Z_{\text{plate}}} + \frac{\phi_{\text{port}}}{Z_{\text{port}}} + \frac{\phi_{\text{leak}}}{Z_{\text{leak}}}\right]^{-1}, \tag{21}$$

where ϕ denotes the filling fraction of each component, Z_{port} is the impedance of the acoustic port including thermosviscous effects [52], and Z_{leak} is the pressure leakage impedance.

To determine the leakage impedance, one can consider the measurement of a rigid or nearly rigid sample without any acoustic ports, in which case the total impedance is simply $Z_{\text{tot}} = Z_{\text{leak}}/\phi_{\text{leak}}$. In the absence of the pressure leakage, all the sound should be reflected and the reflectance should be unity; however, in the presence of the leakage, the measured reflection coefficient for a rigid or nearly rigid sample R_{meas} will exhibit a reduction in the magnitude (and a phase difference as well). An expression for the leakage effects can be obtained using Eq. (19) in terms of the measured complex reflection coefficient R_{meas} as

$$\frac{Z_{\text{leak}}}{\phi_{\text{leak}}} = \frac{2Z_0 R_{\text{meas}}}{1 - R_{\text{meas}}}. \tag{22}$$

Samples consisting of silica aerogel disks measuring 2.43 cm in diameter and 1.1 cm thick are tested in a 3.5-cm-diameter air-filled acoustic impedance tube, as pictured in Fig. 2(b). The acoustic impedance tube used in this work consists of a circular tube having an inner diameter of 3.5 cm. To mount the silica aerogel disks in the impedance tube, wooden rings are machined to support the aerogel disks and provide an acoustic baffle. Because of the brittleness of the aerogel disks, the holes are drilled into the wooden ring to create the acoustic ports, each with a diameter of 1 mm. To obtain the acoustic characterization of the aerogel samples, broadband noise is generated using an electromechanical driver at one end of the tube and measured using 0.50-in- (1.27-cm-) diameter G.R.A.S. condenser pressure microphones. The microphones are arranged in a standard four-microphone configuration [48], allowing for the reflection and transmission pressure coefficients to be directly determined using a transfer-matrix technique [49]. An approximately 1-m-long section of the terminating end of the impedance tube is filled with fiberglass insulation to provide an anechoic termination. This setup was previously demonstrated to provide sufficient reduction in the reflected waves from the terminating end and facilitate accurate extraction of effective acoustic properties [19]. From this set of measurements, the complex impedance and wave number are obtained for the range 300–2000 Hz, in a similar manner to previous experimental work on acoustic metamaterial samples [19,51].

V. RESULTS

The experimental data for the reflectance are shown in Figs. 3(a)–3(c), with the corresponding transmittance data shown in Figs. 3(d)–3(f), for the nominal aerogel sample plus with one and two acoustic ports, respectively. These measured values are relatively constant with frequency except in the vicinity of 1500 Hz, where there is a rapid decrease in reflectance with a corresponding increase in the transmittance due to the flexural resonance of the circular aerogel disk. This anomalous increase in the transmission of acoustic energy in the experimental data far exceeds that expected based on quasistatic homogenization theory for

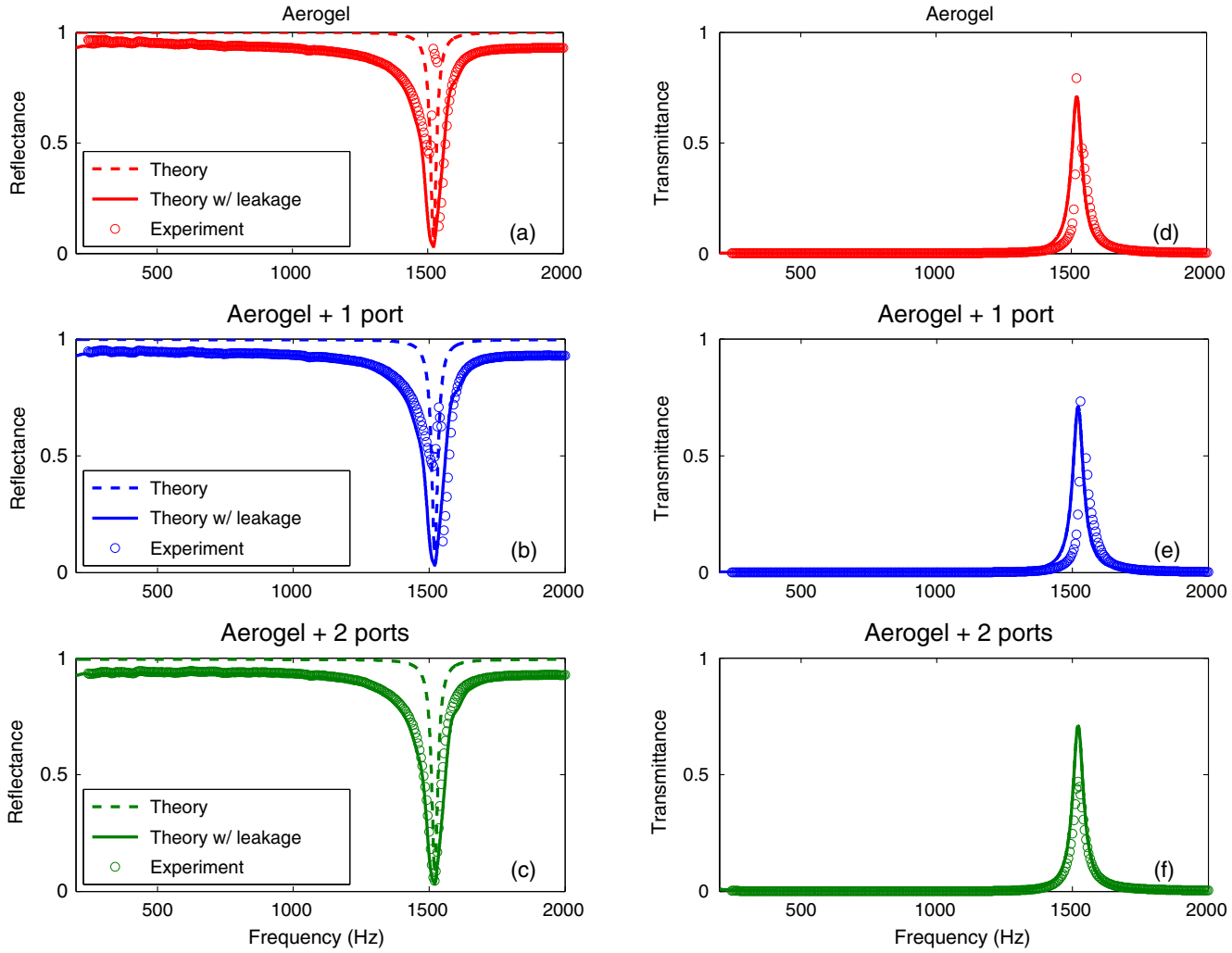

FIG. 3. Comparison of experimental data with the theoretical model presented in Sec. III for the acoustic reflectance (a)–(c) and transmittance (d)–(f). As described by the legend, experimental data are denoted by circles, and the theoretical results are presented with and without corrections due to the pressure leakage through the microphones denoted by the solid and dashed lines, respectively. The properties of the aerogel used in the calculations are given in Table I using a loss factor of 0.005.

such a large impedance contrast with the surrounding air and corresponds to a region of extraordinary transmission.

At the flexural resonance, the magnitude of the reflectance theoretically approaches zero in the absence of losses, although this minimum in reflectance is limited to small but nonzero values when losses in the aerogel are included, as observed in Figs. 3(a)–3(c). This trend is also observed in the experimental results and, overall, is in very good agreement with the theory, although a few spurious data points near the flexural resonance in Figs. 3(a) and 3(b) can be seen in the reflectance data that deviate significantly from those of the model. These particular data points are concentrated in the immediate vicinity of the flexural resonance and are likely due to the complicated interaction between the pressure leakage term and flexural motion of the disk near resonance. This interaction is in agreement with the fact that the significant deviation of these points from the expected value is seen only in the reflectance data (where the pressure leakage effects are observed), while showing very good agreement in the transmittance data.

Based on the measured data, the flexural resonance frequency is obtained, and the Young's modulus of the aerogel sample can be obtained based on the theoretical expression for the resonance frequency given by Eq. (15). The measured properties of the aerogel sample examined in this work are tabulated in Table I. While these measured

TABLE I. Measured values for the flexural resonance frequency, Young's modulus E, and density ρ for the silica aerogel examined in this work. The loss factor of the aerogel is observed to be 0.005 based on the reflectance and transmittance data presented in Fig. 3. The Poisson's ratio is estimated to be 0.21 based on Gross *et al.* [43].

f_{res} (Hz)	E (MPa)	ρ (kg/m^3)
1420	0.569	107

values are somewhat lower than some other similar aerogel samples [43], the results reported here fall within the accepted range of measured aerogel properties [30].

The loss factor of the aerogel is assumed to be a constant over the frequency range examined in this work and is determined from the power absorption coefficient $\alpha = 1 - R^2 - T^2$ at the flexural resonance frequency. Using the absorption coefficient, the experimentally observed losses can be related to the reflection and transmission coefficients, and with the use of Eqs. (19) and (20), they can, therefore, be related to the properties of the aerogel disk through the impedance given by Eq. (18). From the experimental results presented in Fig. 3, the loss factor of each aerogel sample is determined to be 0.005.

From these measured values, an elastic model based on the theoretical formulation presented in Sec. III is calculated and compared to the data. The modeled results obtained without accounting for the pressure leakage effects are denoted by the dashed line in Figs. 3 and 4. While there is excellent agreement with the transmittance shown in Figs. 3(d)–3(f), the theoretical reflectance shown in Figs. 3(a)–3(c) predicts unity away from the flexural resonance, a value which is not observed in the measurements. While this difference between the modeled and measured values represents less than a 10% error over most of the frequency band under investigation, this leads to a significant variation in the resulting extracted effective acoustic properties, as illustrated in Fig. 4. This variation is particularly large below the flexural resonance frequency, for which the variation between the theoretical model without accounting for the leakage differs by up to an order of magnitude from that observed in the experimental data.

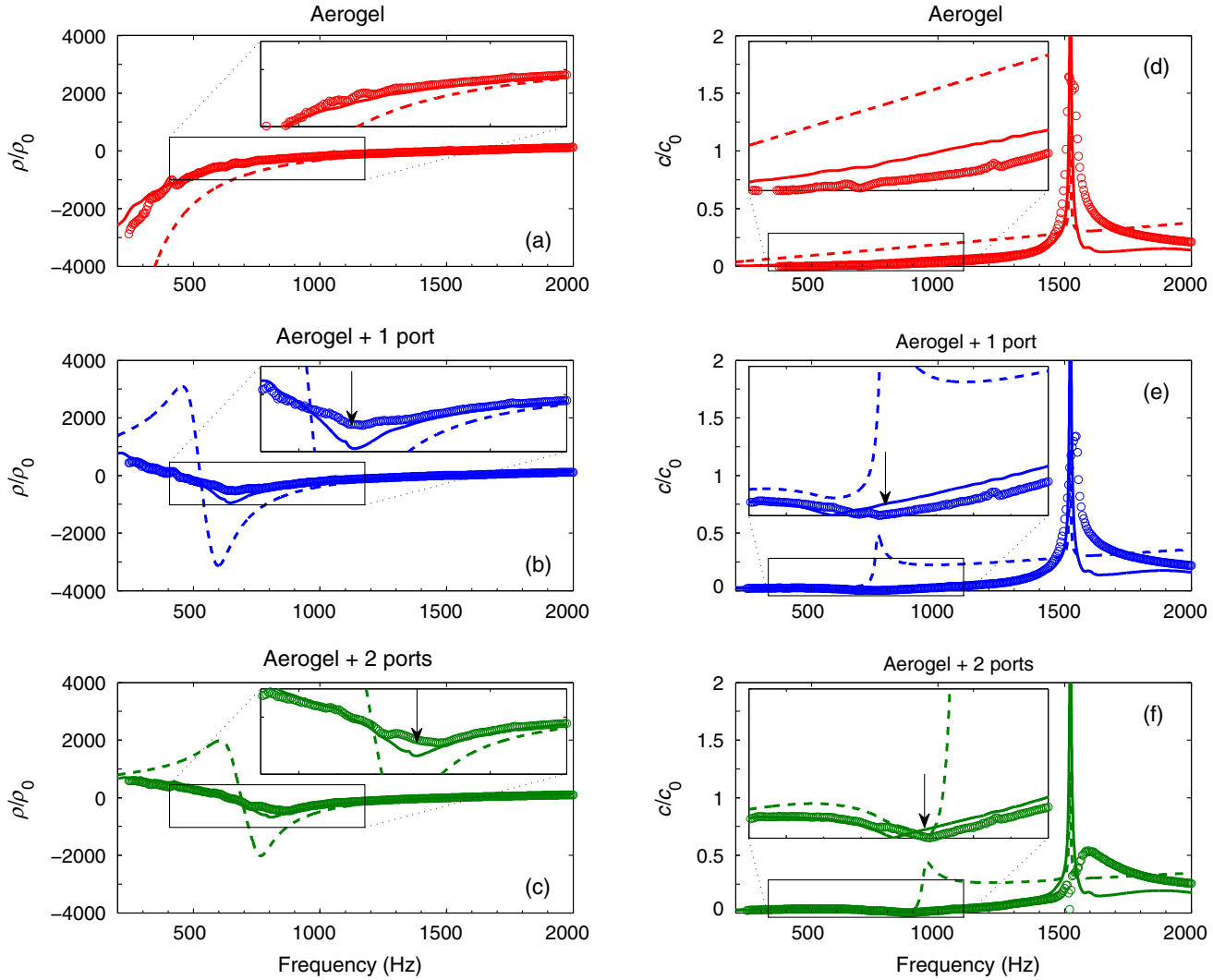

FIG. 4. Comparison of experimental data with the theoretical model presented in Sec. III normalized relative to the properties of air ($\rho_0 = 1.21$ kg/m^3, $c_0 = 343$ m/s) for the effective density (a)–(c) and effective sound speed (d)–(f). The legend is the same as in Fig. 3, in which the experimental data are denoted by circles, and the theoretical results are presented with and without corrections due to the pressure leakage through the microphones denoted by the solid and dashed lines, respectively. The arrows denote extreme values, namely, the peak negative density in (b) and (c) and near-zero slow-sound propagation in (e) and (f).

Accounting for the leakage through the use of Eqs. (21) and (22), this observed difference in the reflectance can be correctly modeled, as shown by the solid lines in Figs. 3 and 4. In addition to the improved agreement in the reflectance presented in Figs. 3(a)–3(c), excellent agreement is also maintained with the transmittance in Figs. 3(d)–3(f). The theoretical model including pressure leakage and the measured data of the extracted effective mass density and sound speed are in excellent agreement, with the model capturing the correct magnitudes and frequency dependence of these dynamic properties. Even with the limitations of the experimental apparatus due to the finite acoustical impedance of the microphones and the resulting acoustic pressure leakage, one is still able to observe an extremely large dynamic range of extracted acoustic properties, on the order of thousands of times that of the ambient air.

In addition to the agreement between the experimental data and theoretical model, the results presented in Fig. 4 provide valuable information regarding the wide range of effective properties which can be attained using the soft acoustic metamaterial arrangement illustrated in Fig. 1. In particular, it can be observed that the overall trends as a function of frequency follow those predicted in Figs. 1(a) and 1(b) for silica aerogel disks with and without parallel arrangements with acoustic ports for the effective mass density and sound speed, respectively. In Fig. 4(a), the effective density for the data obtained for the silica aerogel disk is observed to be positive above the flexural resonance frequency (around 1500 Hz), passing through zero, and then negative below the flexural resonance frequency and tending towards $-\infty$ as frequency decreases. Conversely, the effective sound speed shown in Fig. 4(d) increases significantly as the effective density passes through zero near the flexural resonance frequency and decreases towards zero as the frequency decreases. These effective properties, which arise from the use of the flexural motion of the silica aerogel as a "hidden degree of freedom" [15] in the otherwise 1D planar arrangement of the acoustic impedance tube, lead to these extreme effective properties which differ greatly from the static properties of silica aerogel.

Likewise, the combination of the negative effective density of the silica aerogel disk with the positive effective density of one (or more) acoustic ports yields much more uniform and less dispersive regions of negative density, which are illustrated in Figs. 4(b) and 4(c) for the case of one and two acoustic ports, respectively. As described above, the parallel arrangement of the silica aerogel disk and the acoustic ports leads to the effective properties being dominated by the acoustic port at lower frequencies, leading to this change in the effective density as a function of frequency over this range below the flexural resonance frequency. In the vicinity of the flexural resonance, however, the effective properties are dominated by the silica aerogel disk, and, therefore, the same density-near-zero region is observed.

Similarly, the effective sound speed is presented in Figs. 4(e) and 4(f) for the case of silica aerogel with one and two acoustic ports, respectively. In the vicinity of the flexural resonance, a similar spike in the effective sound speed is observed (corresponding to the effective density passing through zero) as was observed for the silica aerogel disk without any acoustic ports. In addition to this, a dip in the effective sound speed is observed well below the flexural resonance, leading to a region of zero and near-zero effective wave speed in the acoustic metamaterial structure. Previous experimental investigations of slow sound have been observed over relatively narrow bands due to the resonant physical mechanisms employed, whereas the results presented in this paper appear to experimentally demonstrate a broad region of nonresonant slow-sound propagation.

Similar trends in the data described above are observed for the silica aerogel disk combined with either one or two acoustic ports. One interesting point of distinction that can be noted is that the addition of more acoustic ports (and, thus, a larger, positive effective acoustic mass) results in an *increase* in the frequency at which the minimum of the negative density and region of slow sound occur. This stands in contrast with traditional resonant acoustic metamaterials, such as those utilizing simple harmonic oscillators, for which the addition of mass tends to *decrease* the resonant frequency and the corresponding frequencies of negative effective density. This difference for the soft acoustic metamaterial arrangement investigated here arises due to the parallel arrangement of the different components, compared with the traditional series arrangement of mass-spring and transmission-line acoustic metamaterials. Although the soft acoustic metamaterials examined in this paprt are limited to relatively simple lumped elements and canonical geometries, this principle can be extended to a wide range of more elegant acoustic elements allowing for a vast range of tunable exotic properties in a compact design and potential use in conformal arrangements.

VI. CONCLUSION

In conclusion, silica aerogel disks are examined theoretically and experimentally as building units of a soft acoustic metamaterial. It is shown that the combination of the flexural motion of the silica aerogel combined with the acoustic mass of one or more ports leads to a configuration with broadband negative dynamic density, density-near-zero regions, and nonresonant broadband slow-sound propagation. The use of silica aerogel as part of a soft acoustic metamaterial structure with subwavelength thickness is examined theoretically and experimentally. Significant challenges are overcome to obtain direct measurements of the effective density and sound speed for such high-impedance metamaterial elements, which is achieved

using an air-filled acoustic impedance tube and correcting for the inherent pressure leakage from the microphones. The experimental measurements are found to be in very good agreement with the expected theoretical results. Unlike acoustic metamaterials utilizing mass-spring resonators, the soft acoustic metamaterials described in this work move beyond this framework by creating the dynamics from the flexural motion of a soft elastic structure, while offering the tunability to achieve a wide range of desirable exotic properties with a single subwavelength element.

ACKNOWLEDGMENTS

This work is supported by the U.S. Office of Naval Research. M. D. G., V. M. G.-C. and J. S.-D. also acknowledge the support by the Spanish Ministerio de Economía y Competitividad, and the European Union Fondo Europeo de Desarrollo Regional (FEDER) through Project No. TEC2014-53088-C3-1-R. The authors wish to acknowledge Encarna G. Villora and Kiyoshi Shimamura for their help in aerogel fabrication and handling.

[1] M. Maldovan, Sound and heat revolutions in phononics, Nature (London) **503**, 209 (2013).
[2] M. Kadic, T. Bückmann, R. Schittny, and M. Wegener, Metamaterials beyond electromagnetism, Rep. Prog. Phys. **76**, 126501 (2013).
[3] T. Brunet, J. Leng, and O. Mondain-Monval, Soft acoustic metamaterials, Science **342**, 323 (2013).
[4] J. Christensen, L. Martin-Moreno, and F. J. Garcia-Vidal, Theory of Resonant Acoustic Transmission through Subwavelength Apertures, Phys. Rev. Lett. **101**, 014301 (2008).
[5] J. J. Park, K. J. B. Lee, O. B. Wright, M. K. Jung, and S. H. Lee, Giant Acoustic Concentration by Extraordinary Transmission in Zero-Mass Metamaterials, Phys. Rev. Lett. **110**, 244302 (2013).
[6] R. Fleury, C. F. Sieck, M. R. Haberman, and A. Alù, Acoustic supercoupling through a density-near-zero metamaterial channel, J. Acoust. Soc. Am. **132**, 1956 (2012).
[7] R. Fleury and A. Alù, Extraordinary Sound Transmission through Density-Near-Zero Ultranarrow Channels, Phys. Rev. Lett. **111**, 055501 (2013).
[8] R. Gracia-Salgado, V. M. García-Chocano, D. Torrent, and J. Sanchez-Dehesa, Negative mass density and density-near-zero quasi-two-dimensional metamaterials: Design and applications, Phys. Rev. B **88**, 224305 (2013).
[9] A. Santillán and S. I. Bozhevolnyi, Acoustic transparency and slow sound using detuned acoustic resonators, Phys. Rev. B **84**, 064304 (2011).
[10] W. M. Robertson, C. Baker, and C. Brad Bennett, Slow group velocity propagation of sound via defect coupling in one-dimensional acoustic band gap array, Am. J. Phys. **72**, 255 (2004).
[11] A. Cicek, O. A. Kaya, M. Yilmaz, and B. Ulug, Slow sound propagation in a sonic crystal linear waveguide, J. Appl. Phys. **111**, 013522 (2012).
[12] A. Santillán and S. I. Bozhevolnyi, Demonstration of slow sound propagation and acoustic transparency with a series of detuned resonators, Phys. Rev. B **89**, 184301 (2014).
[13] G. Theocharis, O. Richoux, V. Romero García, A. Merkel, and V. Tournat, Limits of slow sound propagation and transparency in lossy, locally resonant periodic structures, New J. Phys. **16**, 093017 (2014).
[14] J.-P. Groby, W. Huang, A. Lardeau, and Y. Aurégan, The use of slow waves to design simple sound absorbing materials, J. Appl. Phys. **117**, 124903 (2015).
[15] G. W. Milton and J. R. Willis, On modifications of Newton's second law and linear continuum elastodynamics, Proc. R. Soc. A **463**, 855 (2007).
[16] D. Torrent, Y. Pennec, and B. Djafari-Rouhani, Effective medium theory for elastic metamaterials in thin elastic plates, Phys. Rev. B **90**, 104110 (2014).
[17] P. Li, S. Yao, and X. Zhou, Effective medium theory for thin-plate acoustic metamaterials, J. Acoust. Soc. Am. **135**, 1844 (2014).
[18] F. Cervera, L. Sanchis, J. V. Sánchez-Pérez, R. Martínez-Sala, C. Rubio, F. Meseguer, C. López, D. Caballero, and J. Sánchez-Dehesa, Refractive Acoustic Devices for Airborne Sound, Phys. Rev. Lett. **88**, 023902 (2001).
[19] M. D. Guild, V. M. Garcia-Chocano, W. Kan, and J. Sánchez-Dehesa, Acoustic metamaterial absorbers based on multilayered sonic crystals, J. Appl. Phys. **117**, 114902 (2015).
[20] N. Fang, D. Xi, J. Xu, M. Ambati, W. Srituravanich, C. Sun, and X. Zhang, Ultrasonic metamaterials with negative modulus, Nat. Mater. **5**, 452 (2006).
[21] F. Bongard, H. Lissek, and J. R. Mosig, Acoustic transmission line metamaterial with negative/zero/positive refractive index, Phys. Rev. B **82**, 094306 (2010).
[22] Y. Xiao, J. Wen, and X. Wen, Sound transmission loss of metamaterial-based thin plates with multiple subwavelength arrays of attached resonators, J. Sound Vib. **331**, 5408 (2012).
[23] M. Oudich, X. Zhou, and M. B. Assouar, General analytical approach for sound transmission loss analysis through a thick metamaterial plate, J. Appl. Phys. **116**, 193509 (2014).
[24] S. H. Lee, C. M. Park, Y. M. Seo, Z. G. Wang, and C. K. Kim, Composite Acoustic Medium with Simultaneously Negative Density and Modulus, Phys. Rev. Lett. **104**, 054301 (2010).
[25] A. Bozhko, V. M. García-Chocano, J. Sanchez-Dehesa, and A. Krokhin, Redirection of sound in straight fluid channel with elastic boundaries, Phys. Rev. B **91**, 094303 (2015).
[26] L. W. Hrubesh, Aerogel applications, J. Non-Cryst. Solids **225**, 335 (1998).
[27] H. Nagahara and M. Hashimoto, in *Aerogels Handbook*, edited by M. A. Aegerter, N. Leventis, and M. M. Koebel (Springer, New York, 2011), Chap. 33.
[28] V. Gibiat, O. Lefeuvre, T. Woignier, J. Pelous, and J. Phalippou, Acoustic properties and potential applications of silica aeogels, J. Non-Cryst. Solids **186**, 244 (1995).
[29] L Forest, V Gibiat, and T. Woignier, Biot's theory of acoustic propagation in porous media applied to aerogels and alcogels, J. Non-Cryst. Solids **225**, 287 (1998).
[30] M. Gronauer and J. Fricke, Acoustic properties of microporous SiO_2-aerogel, Acta Acust united Ac. **59**, 177 (1986).

[31] Z. Liu, X. Zhang, Y. Mao, Y. Y. Zhu, Z. Yang, C. T. Chan, and P. Sheng, Locally resonant sonic materials, Science **289**, 1734 (2000).

[32] C. J. Naify, C.-M. Chang, G. McKnight, and S. Nutt, Transmission loss and dynamic response of membrane-type locally resonant acoustic metamaterials, J. Appl. Phys. **108**, 114905 (2010).

[33] C. J. Naify, C.-M. Chang, G. McKnight, F. Schuelen, and S. Nutt, Membrane-type metamaterials: Transmission loss of multi-celled arrays, J. Appl. Phys. **109**, 104902 (2011).

[34] G. Ma, M. Yang, Z. Yang, and P. Sheng, Low-frequency narrow-band acoustic filter with large orifice, Appl. Phys. Lett. **103**, 011903 (2013).

[35] Y. Chen, G. Huang, X. Zhou, G. Hu, and C. T. Sun, Analytical coupled vibroacoustic modeling of membrane-type acoustic metamaterials: Plate model, J. Acoust. Soc. Am. **136**, 2926 (2014).

[36] D. Torrent and J. Sánchez-Dehesa, Multiple scattering formulation of two-dimensional acoustic and electromagnetic metamaterials, New J. Phys. **13**, 093018 (2011).

[37] C. J. Naify, C. N. Layman, T. P. Martin, M. Nicholas, D. C. Calvo, and G. J. Orris, Experimental realization of a variable index transmission line metamaterial as an acoustic leaky-wave antenna, Appl. Phys. Lett. **102**, 203508 (2013).

[38] D. T. Blackstock, *Fundamentals of Physical Acoustics*, 1st ed. (John Wiley & Sons, New York, 2000).

[39] K. F. Graff, *Wave Motion in Elastic Solids* (Dover Publications, New York, 1975).

[40] H. Lee and R. Singh, Acoustic radiation from out-of-plane modes of an annular disk using thin and thick plate theory, J. Sound Vib. **282**, 313 (2005).

[41] C. D. Hettema, Ph.D. thesis, Naval Postgraduate School, 1988.

[42] M. Abramowitz and I. A. Stegun, *Handbook of Mathematical Functions: With Formulas, Graphs and Mathematical Tables* (Dover, New York, 1972).

[43] J. Gross, G. Reichenauer, and J. Fricke, Mechanical properties of SiO_2 aerogels, J. Phys. D **21**, 1447 (1988).

[44] T. E. Gómez Álvarez Arenas, F. R. Montero de Espinosa, M. Moner-Girona, E. Rodriguez, A. Roig, and E. Molins, Viscoelasticity of silica aerogels at ultrasonic frequencies, Appl. Phys. Lett. **81**, 1198 (2002).

[45] H. Lu, H. Luo, and N. Leventis, in *Aerogels Handbook*, edited by M. A. Aegerter, N. Leventis, and M. M. Koebel (Springer, New York, 2011), Chap. 22.

[46] Y. Xie and J. R. Beamish, Ultrasonic properties of silica aerogels at low temperatures, Phys. Rev. B **57**, 3406 (1998).

[47] J. A. Rogers and C. Case, Acoustic waveguide properties of a thin film of nanoporous silica on silicon, Appl. Phys. Lett. **75**, 865 (1999).

[48] Y. Salissou and R. Panneton, Wideband characterization of the complex wave number and characteristic impedance of sound absorbers, J. Acoust. Soc. Am. **128**, 2868 (2010).

[49] B. H. Song and J. S. Bolton, A transfer-matrix approach for estimating the characteristic impedance and wave numbers of limp and rigid porous materials, J. Acoust. Soc. Am. **107**, 1131 (2000).

[50] V. Fokin, M. Ambati, C. Sun, and X. Zhang, Method for retrieving effective properties of locally resonant acoustic metamaterials, Phys. Rev. B **76**, 144302 (2007).

[51] M. D. Guild, V. M. Garcia-Chocano, W. Kan, and J. Sánchez-Dehesa, Enhanced inertia from lossy effective fluids using multi-scale sonic crystals, AIP Adv. **4**, 124302 (2014).

[52] L. E. Kinsler, A. R. Frey, A. B. Coppens, and J. V. Sanders, *Fundamentals of Acoustics*, 4th ed. (John Wiley & Sons, New York, 2000).